Proceedings of the 1st Global Power and Propulsion Forum
GPPF 2017
Jan 16-18, 2017, Zurich, Switzerland
www.pps.global

GPPF-2017-78

EXPLORATORY ASSESSMENT OF A COMBINED-CYCLE ENGINE CONCEPT FOR AIRCRAFT PROPULSION

C. M. De Servi, L. Azzini, M. Pini, A. Gangoli Rao, P. Colonna
Propulsion and Power
Aerospace Engineering Faculty
Delft University of Technology
Kluiyverweg 1
2628 CD Delft
The Netherlands
Corresponding author: p.colonna@tudelft.nl

ABSTRACT

This preliminary study considers a combined cycle configuration for aeroengines, whereby thermal energy from the exhaust of the gas turbine is partly recovered in order to obtain additional mechanical power. The waste heat recovery system is based on a closed thermodynamic bottoming cycle with supercritical carbon dioxide ($scCO_2$) as working fluid, allowing to achieve a very high power density. As first step of the investigation a thermodynamic cycle analysis of the combined-cycle engine (CCE) is carried out. Results are compared to those of the intercooled-recuperative engine (IRE) configuration for the same operating conditions and calculated under the same modeling assumptions. The estimated nominal SFC of the proposed CCE configuration is approximately 20% lower compared to that of a conventional turbofan, and 6% lower than that of the IRE, if pressure drops in the heat exchangers are neglected.

Such large gain justified further analysis, by including the preliminary sizing of main components. Once the sizing of heat exchangers is factored in, the thermodynamic benefit of the CCE is offset by the penalty due to the weight of the additional equipment. This is mainly caused by i) the space constraints of the turbofan nacelle, which strongly limit the recoverable thermal power, and ii) the lack of proper het exchanger technology for such a highly unconventional application.

These issues, and the many other that need consideration, will be addressed in an upcoming research project encompassing a much wider scope involving new aircraft and propulsion system configurations.

1 INTRODUCTION

Currently, technological improvements affecting aero-engine efficiency are mainly targeted to incremental increase of turbomachinery performance, engine turbine inlet temperature (TIT) rise, and larger overall pressure ratio (OPR). Long-range turbofan engines commercially available between year 1990 and 2010 featured a TIT increase from 1600 K to 1800 K, along with an almost doubling of the by-pass ratio (BPR) and an increment of the OPR from 35 to more than 50. These developments led to an overall engine efficiency of up to 37%, with an yearly average increment of approximately 0.5% [1]. However, it is debatable whether the current improvement in TIT (10K/year) can be sustained in the future [2]. Moreover, higher TIT values imply a rise in NO_x emissions. Thus, the aerospace industry is exploring novel propulsion system configurations in order to reduce the environmental footprint of civil aviation.

Heat recovery from engine exhaust is a technical option that may enable significant reduction of specific fuel consumption (SFC) as well as emissions. In a modern aircraft turbofan, wasted thermal power accounts for 50-55% of the fuel energy input. A fraction of this waste energy can be exploited to preheat the combustion air or converted into usable power by means of a prime mover. The first option, the so-called recuperated aero-engine configuration has been investigated since the 1940's. As reported

by Mc Donald et al. [3], these research efforts led in the 60's to the realization of the first prototypes for military applications, i.e. the Lycoming T53 turboshaft and the Allison T78 turboprop; the thermal power extracted from exhaust amounted to 820 kW_{th} and 3080 kW_{th}, respectively. The research following such early studies focused on the development of the intercooled-recuperated engine (IRE) concept. The most recent research results about the IRE show that a SFC reduction of 2% is arguably achievable by redesigning the engine and using compact heat exchangers (HEXs) [4, 5].

Engine waste heat recovery (WHR) has been considered only recently. The study described in Ref. [6] is related to a Combined Cycle Engine (CCE) consisting of a turbofan equipped with a bottoming organic Rankine cycle (ORC) unit supplying additional mechanical power to the high-pressure compressor of the engine and electrical power to the aircraft avionics. The total power output of the WHR system is around 200 kW. The predicted SFC reduction with respect to the SFC of the base case is approximately 2.3%, if pressure drops in the heat exchangers of the ORC unit and the impact of the additional system weight on the required thrust are neglected.

The study documented here examined the viability of a different CCE configuration, whereby the energy content of the gas turbine exhaust is recovered by means of a system based on the supercritical carbon dioxide ($scCO_2$) power cycle concept, see, e.g. [7, 8]. The main advantages of this concept, initially conceived for terrestrial applications, are the very high power density, the thermal stability of the working fluid, and, consequently, the high conversion efficiency that can be achieved.

In order to explore the potential of the proposed solution, first a thermodynamic analysis of the CCE has been performed, and the results compared with a similar analysis carried out on an IRE operating at the same conditions, and for which validated data are available in the literature. Subsequently, the effect of actual equipment on the performance of the engine has been assessed by assuming that the WHR unit is added to a common modern turbofan engine, the GE90-94B. The primary heat exchanger of the $scCO_2$ power system is inserted after the low-pressure turbine, in the core nozzle, while the cooler is placed in the fan duct. Even though such configuration is not representative of the future aircraft for which the CCE is conceived, and related design restrictions heavily penalize the achievable performance, the availability of actual data related to the main engine allowed for a WHR unit preliminary design based on verifiable assumptions. The results of this analysis provide therefore a lower boundary for the achievable performance, and can be used as a starting point for further investigation.

2 THERMODYNAMIC CYCLE CONFIGURATION AND SIMPLIFIED PERFORMANCE ANALYSIS

In a $scCO_2$ closed Brayton cycle the compression process occurs with the fluid at thermodynamic states close to the vapor-liquid critical point, thus greatly reducing the fraction of turbine work needed to power the compressor, if compared to a conventional gas turbine cycle. Given the small temperature drop experienced by CO_2 over the expansion in the turbine, high thermodynamic efficiency can only be achieved if the thermal energy at the turbine exhaust is used to preheat the working fluid entering the primary heat exchanger. Various configurations are currently studied [9] and implemented in the first prototypes and pre-commercial units for terrestrial applications [10].

The simplest regenerated cycle configuration has been selected for this exploratory study, see Fig.1. With reference to thermodynamic state points in Fig. 1a, CO_2 is heated by the turbofan exhaust gas from state $2a_{WHR}$ to state 3_{WHR}, and then it expands in the turbine from state 3_{WHR} to 4_{WHR}. Subsequently, the working fluid is cooled in the regenerator down to the temperature of state $4a_{WHR}$ in order to preheat the CO_2 from the outlet of the compressor (state 2_{WHR}) up to the temperature of state $2a_{WHR}$. Finally, the working fluid at the cold outlet of the regenerator is further cooled down to the cycle minimum temperature (state 1_{WHR}), and compressed from close-to-critical conditions up to the maximum cycle pressure of state 2_{WHR}.

In order to assess the potential of the CCE concept at coarse level, first the thermodynamic performance of a CCE is calculated by means of a simplified simulation and compared to that of an IRE for the same operating conditions and under the same simplifying assumptions. It is therefore assumed that

- the engine operates in stationary cruise conditions (design point), for a given gas turbine engine TIT, BPR, and fan pressure ratio (FPR);
- the effect of weight and size of the equipment on the specific fuel consumption is neglected;
- the effect of the heat exchangers on the overall performance is simply modeled by means of two parameters, namely the number of thermal units NTU, and the pressure drops ΔP on the cold and hot side , which are assumed proportional to the total pressure of the stream at the HEX inlet. The number of thermal units is evaluated as $\mathrm{NTU} = \frac{UA}{C_{\min}}$, where U is the global heat transfer coefficient, A the heat transfer area, and $C_{\min}$ the value of the minimum heat capacity among those of the two flows;
- the design parameters of the CCE and IRE engines are those listed in Tables 1, 2, and 3. Performance values related to the gas turbines are selected so as to be representative of current technology. Performance values related to the $scCO_2$ WHR unit follow the recommendations in Ref. [7];

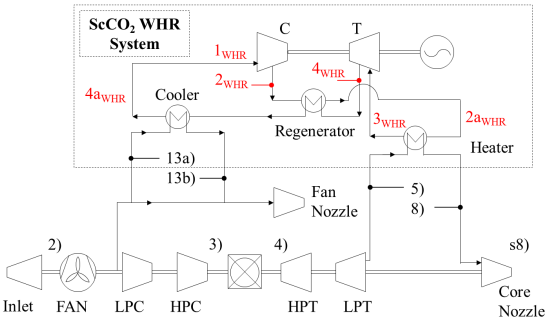

(a) Simplified process flow diagram

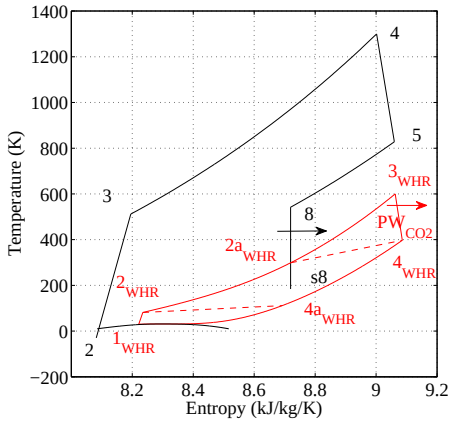

(b) Thermodynamic cycles in the $T-s$ diagram of CO_2. The values of specific entropy of the state points related to the gas turbine engine cycle have been scaled appropriately in order to correctly correspond to the pertinent $scCO_2$ cycle state points, thus neglecting that they refer to different working fluids.

FIGURE 1. Combined-cycle aero engine adopting a $scCO_2$ cycle unit for heat recovery from the gas turbine exhaust.

- the mechanical power obtained from the $scCO_2$ WHR unit is converted into thrust with the same efficiency as that obtained from the gas turbine, namely 90%;
- the value of the intercooler pressure for the IRE configuration is taken equal to the square root of the OPR value times the inlet engine pressure, so as to approximate the optimal value.

The steady state modeling of the gas turbines under these assumptions is performed with a well-known object-oriented simulation environment for 0D modeling of gas turbines [11], which has been extensively validated and successfully used over the years to predict the performance of many aero-engines and power plants [12]. The software was developed from the late '80s and is at present the NLRs primary tool for gas turbine engine performance analysis.

TABLE 1. Model specifications for the gas turbines

Air mass flow rate (kg/s)	500
TIT(K)	1,500
BPR (-)	9.0
FPR (-)	1.4
Cruise Altitude (m)	10,000
Cruise Mach number (-)	0.8
Fan efficiency (%)	90
Compressor efficiency (%)	89
Turbine efficiency (%)	91

TABLE 2. Model specifications for the IRE and the CCE

$NTU_{heater/recuperator}$	1 - 4
$NTU_{cooler/intercooler}$	$= NTU_{heater/recuperator}$
$(\Delta P/P_{inlet})_{HEX}$	0 - 0.1
OPR	5 - 115
$\dot{m}_{coolant}$	$= \dot{m}_{air,core}$

TABLE 3. Model specifications for the $scCO_2$ WHR unit

$\Delta T_{pinch,regenerator}$ (K)	15
$(\Delta P/P_{in})_{regenerator}$ (%)	2
T_{min} (K)	283
P_{max} (MPa)	10 - 40
P_{min} (MPa)	7.4
Compressor efficiency (%)	85
Turbine efficiency (%)	90
η_{prop,CO_2} (%)	90

The simulation of the CCE required the development of a program implementing the model of the $scCO_2$ WHR unit, which was coded in a widely adopted technical computing environment [13]. The gas turbine and the $scCO_2$ WHR unit models are coupled thanks to the application programming interface (API) available within the gas turbine simulation program. The model of the $scCO_2$ system has been validated by comparison with data reported in Ref. [8] for several $scCO_2$ cycle configurations.

In order to evaluate the influence of the heat exchangers performance on the efficiency of the CCE, simulations are carried out by varying i) the value of NTU of the heat exchangers in the range from 2 to 4, and, ii) the value of the proportionality constant of the pressure losses between 0% and 6%.

Another parameter that is expected to significantly affect the performance of the CCE is the OPR of the gas turbine engine, similarly to what is observed for combined cycle gas turbine (CCGT) power plants. For this reason, simulations are also performed whereby the pressure ratio of the gas turbine engine is varied from OPR = 5 to OPR = 115. Such a wide range is adopted

because the optimal OPR value is not known a priori, as opposed to the case of the IRE, which has already been investigated extensively in the literature [2,14]. In order to take into account the dependence of the mass flow rate of bleed air required for turbine blade cooling from the engine OPR, a correlation calibrated on the data reported in Ref. [15] has been adopted.

Given the specifications listed in Tables 1-3, the main design variables of the $scCO_2$ WHR system are the minimum and the maximum cycle pressures (P_{min}, P_{max}), and the minimum temperature (T_{min}) reached by the working fluid in the cooler. P_{min} is set to 7.4 MPa, a value just above the critical pressure of CO_2, namely 7.36 MPa, while T_{min} is arbitrarily assumed equal to 283 K. P_{max} is a degree of freedom for the design of the WHR unit, and it can be set to the value that minimizes the SFC of the engine. The optimization is therefore constrained with an upper limiting value $P_{max} = 40$ MPa, in line with the state-of-the-art technology of modern steam power plants. The cooler of the $scCO_2$ unit as well as the intercooler of the IRE use as coolant a portion of the air mass flow rate discharged by the engine fan ($\dot{m}_{coolant}$). Notably, in this analysis the amount of cooling air is arbitrarily taken equal to the air mass flow rate of the engine core for both the IRE and the CCE configurations.

2.1 Results

The first relevant information that can be inferred from the results of the thermodynamic cycle analysis is that, in this simplified case, the optimal $scCO_2$ cycle is that featuring the maximum thermal efficiency, which is achieved for the maximum allowable pressure $P_{max} = 40$ MPa. This is contrary to what is known for conventional WHR systems for stationary applications, whereby the optimal pressure level is always the result of a trade-off between i) the thermal efficiency of the bottoming cycle and ii) the amount of energy that is fed to the bottoming cycle [8]. This difference can be explained in light of the fact that i) in a CCE the thermal power which is not recovered from the turbofan exhaust is not completely wasted because it is partially converted into thrust in the engine core nozzle, and ii) the efficiency of this conversion process is relatively high.

Specific fuel consumption. Figure 2 shows values of SFC as a function of OPR and heat exchangers NTU calculated for the CCE, the IRE and a simple-cycle engine (indicated as baseline case in the figure). The pressure drop over the heat exchangers is neglected. The value of SFC estimated for the CCE is markedly lower that that of the simple-cycle engine over the entire OPR range, and the minimum SFC value is lower than the minimum SFC value calculated for the IRE. The best performance is computed for a pressure ratio of approximately 80 for both the CCE and the baseline case, while in case of the IRE the optimal value is obtained at much lower OPR. Interestingly, the SFC-OPR lines related to the CCE and the baseline case display the same trend, which suggests that the considered engine configuration can be attractive also considering the likely evolution of gas turbine technology.

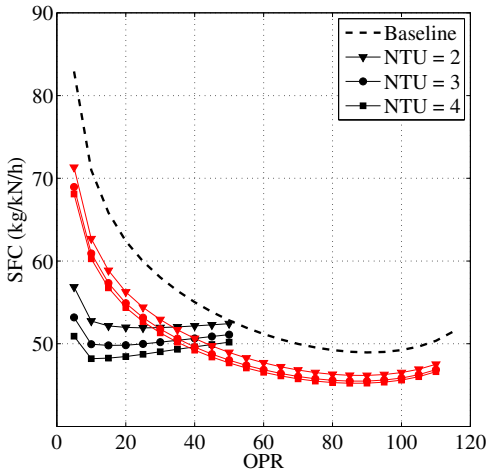

FIGURE 2. **Calculated SFC for the IRE (black), the CCE (red) and baseline case (dotted line). $\Delta P = 0$ for the heat exchangers.**

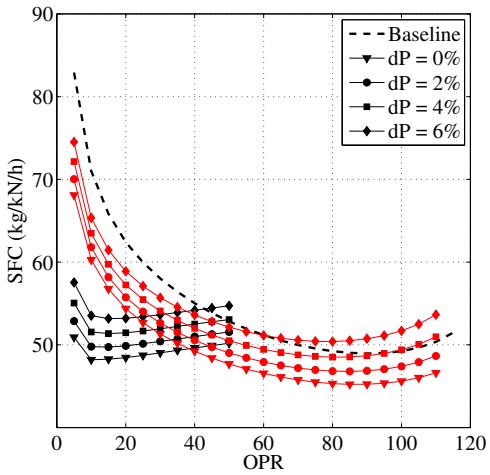

FIGURE 3. **Calculated SFC for the IRE (black), the CCE (red) and the baseline case (dotted line). NTU = 4 for the heat exchangers.**

Figure 3 shows that, as expected, if friction losses in the heat exchangers are taken into account, the calculated performance of the CCE reduces considerably. The estimated SFC becomes larger with increasingly higher pressure drop in the engine core nozzle and in the fan duct. As opposed to the IRE, such trend is more pronounced at high OPR values, thus shifting the position of the minimum SFC value towards lower pressure ratios. The thermodynamic advantage of recovering thermal energy from the gas turbine vanishes for OPR = 60 and $\Delta P/P_{HEX,inlet} = 6\%$ (relative heat exchanger pressure drop). This value of relative pressure drop can be taken as initial value for the maximum pressure

loss in the thermo-hydraulic design of the heat exchangers.

Heat Exchangers. Another important aspect which can be deduced from Fig.2 is that the estimated performance of the CCE is much less sensitive to the NTU value of the heat exchangers than that of the IRE. The SFC of the CCE decreases by a few percentage points for NTU values decreasing from 4 to 2, while the SFC estimated for the IRE rapidly deteriorates for the same variation of the NTU values, especially for low OPR values. Although no general conclusion can be drawn unless all components are reliably sized, these computations suggest that the CCE might require less bulky heat exchangers in comparison to the IRE, thus allowing for lower pressure drops in the gas turbine exhaust and in the fan duct. The charts of Fig. 4 and 5, reporting the calculated thermal power transferred in the cooler and heater as a function of the OPR for both the CCE and the IRE, hint at a similar outcome. This simplified analysis shows that the thermal duty of the IRE heat exchangers is in general larger that that of the corresponding heat exchangers of the CCE. The result can be explained by considering that the $scCO_2$ cycle features internal regeneration, which reduces the thermal load of the cooler and the heater, increasing at the same time the cycle efficiency. The thermal power transferred in the regenerator is a significant fraction of the total thermal energy needed to heat CO_2 to the maximum cycle temperature and it can be even higher than the thermal duty of the heater and the cooler (Fig. 6). Nonetheless, the estimated total thermal duty of the heat exchangers of the CCE, including that the regenerator, is lower than total thermal duty computed for the heat exchangers of the IRE for any given OPR value. If such a comparison is carried out for the optimal pressure ratio calculated for the two engine types, i.e., $\mathrm{OPR}_{\mathrm{IRE}} = 15$ and $\mathrm{OPR}_{\mathrm{CCE}} = 80$, the difference in the total thermal duty of the heat exchangers is eben largest.

Cooling air mass flow rate. Figure 4 reveals that the thermal power exchanged by the cooler of the CCE does not vary with the OPR of the gas turbine, as it is only a function of the mass flow rate assumed for the cooling air ($\dot{m}_{\mathrm{coolant}}$) and of the assumed NTU value. The mass flow rate of cooling air strongly influences the performance of the WHR unit as it affects the CO_2 mass flow rate and consequently the maximum amount of thermal energy that can be recovered. In order to allow for further insight about the relevance of the amount of cooling air mass flow rate, Fig. 7 displays the calculated SFC of the CCE for $\dot{m}_{\mathrm{coolant}} = 2\dot{m}_{\mathrm{core}}$, and zero pressure drop in the heat exchangers. The increase of $\dot{m}_{\mathrm{coolant}}$ determines a significant improvement in the estimated efficiency of the CCE. For a gas turbine engine with OPR equal to 80, the estimated SFC is almost 7% lower than the minimum SFC value reported in Fig. 2. Moreover, the minimum SFC is computed for higher OPR values. However, it must be remarked that the values in Fig. 2 are calculated without taking into account the decrease of fan thrust caused by the larger friction losses in the fan duct, which are proportional to the mass flow rate of cooling air diverted to the cooler. The thermal power

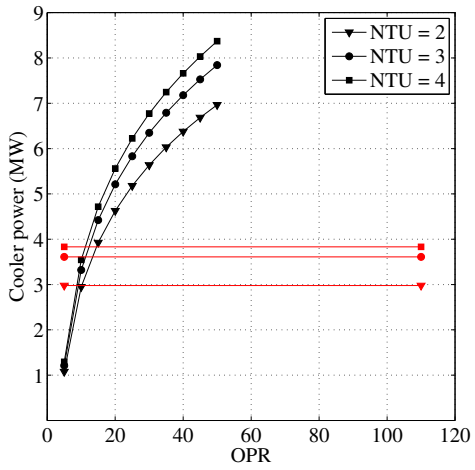

FIGURE 4. **Calculated thermal power exchanged in the cooler of the IRE (black) and of the CCE (red). $\Delta P = 0$ over both sides of the heat exchanger.**

transferred by the cooler in the fan duct is arguably insufficient to compensate for the thrust loss due to the pressure drop on the air side.

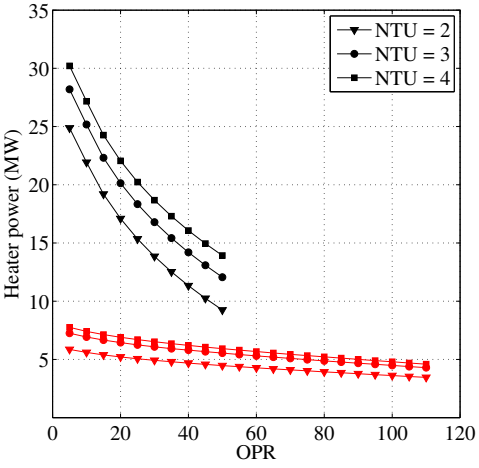

FIGURE 5. **Calculated thermal power exchanged in the heater of the IRE (black) and of the CCE (red). $\Delta P = 0$ over both sides of the heat exchanger.**

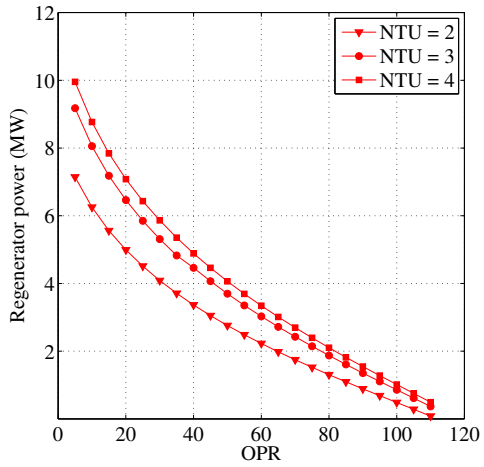

FIGURE 6. **Calculated thermal power exchanged in the regenerator of the $scCO_2$ WHR unit. $\Delta P = 0$ over both sides of the heat exchanger.**

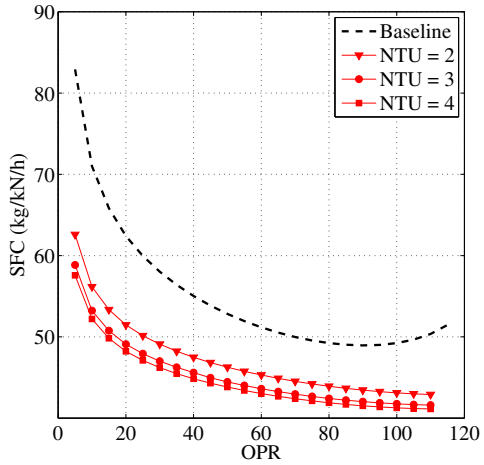

FIGURE 7. **Estimated SFC for the CCE (red) and the baseline case (dotted line) assuming $\dot{m}_{\text{coolant}} = 2\dot{m}_{\text{core}}$. $\Delta P = 0$ over both sides of the heat exchanger.**

3 THE $scCO_2$ POWER SYSTEM AS WASTE HEAT RECOVERY ADD-ON UNIT FOR THE GE90-94B TURBOFAN ENGINE

Realistic, though approximated, optimal design parameters for the $scCO_2$ cycle cannot be determined, unless the position of the heat exchangers within the nacelle or other location in the aircraft is carefully selected and modeled, and all system components correctly sized within a global system optimization procedure. Locating the power plant in a nonconventional position within the aircarft would imply the complete redesign of the vehicle. The preliminary design of a $scCO_2$ unit conceived as add-on to the GE90-94B engine was performed as a first learning step, and as a probing exercise. On the one hand, the adoption of an existing turbofan configuration implies that the preliminary design of the heat exchangers is based on established data. On the other, this information not representative of the level of gas turbine technology suiting this possible development, which targets the mid-term future.

As shown in Fig. 8, also in this case the heater of the $scCO_2$ WHR system is assumed to be located in the engine core nozzle. The cooler is positioned in the fan duct where part of the air flow at the fan outlet is diverted toward it in a separate channel. With reference to Fig. 9, the cooling air first flows through a diffuser in order to reduce the flow velocity, thus the pressure drops in the cooler. Downstream of the cooler, air is irreversibly mixed with the main air stream from the fan, before being discharged into the atmosphere through the fan nozzle. As far the regenerator of the $scCO_2$ unit is concerned, it is assumed that this component can be located in the aircraft fuselage.

3.1 System modeling and design

The method developed during this study to address the preliminary design of the considered CCE configuration deals for simplicity with a single design point, corresponding to a cruise condition. The procedure consists of six main steps:

1. the thermodynamic state points of the turbofan gas turbine cycle are recalculated from available data using a model coded in the in-house gas turbine simulation tool [12]. The pressure drop over the fan duct and heat transfer through bounding surfaces are neglected;
2. the specific thermodynamic properties of CO_2 at the state points of the cycle are estimated by means of the usual mass and energy balances;
3. the preliminary design of the cooler is carried out, together with the estimation of the CO_2 mass flow rate and the cooling air, by solving a non-linear system of equations;
4. the heater is sized according to a preliminary design procedure similar to that adopted for the cooler;
5. the overall thrust of the CCE is then evaluated, taking into account the reduction in the turbofan thrust due to the cooling of the gas turbine exhaust and the pressure drop in the heat exchangers. A simulation of the turbofan engine is run, this time with values of these penalties as additional inputs. Also in this case, it is assumed that the power output of the $scCO_2$ WHR unit can be converted into thrust with 90 % efficiency;
6. finally, the preliminary design of the regenerator is carried out and the total weight of the $scCO_2$ cycle components is estimated.

TABLE 4. Main characteristics and performance of the GE90-94B turbofan at cruise conditions.

Dry weight (kg)	7,550
Cruise Thrust (kN)	70.6
TIT (K)	1,446
Inlet mass flow rate (kg/s)	532.6
By pass ratio (-)	9.0
OPR (-)	41.7
SFC (kg/kNh)	56.3
Cruise Altitude (m)	10,670
Cruise velocity (m/s)	237.2
Auxiliary power (kW)	300

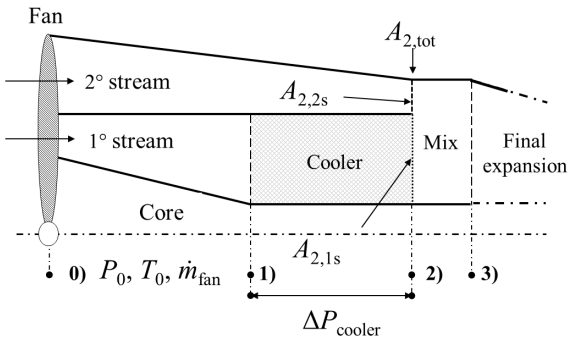

FIGURE 9. Schematic diagram of the layout of the fan duct.

In this simplified design method, the impact of the weight of the WHR unit on fuel consumption due to the required additional thrust is neglected. This effect is qualitatively assessed a posteriori, by assuming, to a first approximation, that the percentage increase of SFC is equal to one tenth of that of the engine weight, as suggested in Ref. [16]. Moreover, the procedure does not include the preliminary sizing of the $scCO_2$ turbo-compressor since its weight is expected to be a small fraction of the total weight.

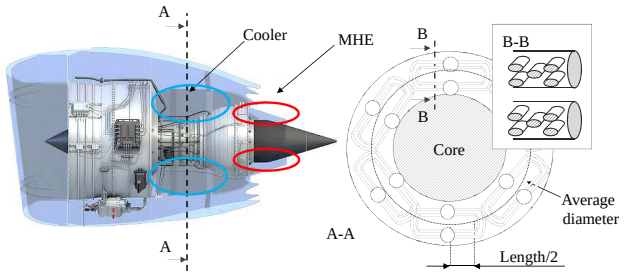

FIGURE 8. Schematic of the modified GE90-94B turbofan engine showing the positioning of the cooler and the heater of the $scCO_2$ waste heat recovery unit and a simplified section and detail of the cooler.

A brief description of the component models follows, in the order in which the design calculations are performed.

Turbofan. The model of the GE90-94B turbofan engine implemented in the in-house gas turbine simulation program has been calibrated by comparison with data available in the open literature for the cruise and take-off operating conditions. The main characteristics of the engine predicted at cruise condition by the model are listed in Table 4.

$scCO_2$ unit. The thermodynamic efficiency and the parameters of the $scCO_2$ cycle are estimated by using the in-house code. No cycle parameters optimization is needed, as, according results presented in Sec. 2, the maximum amount of energy is recovered by the cycle featuring the highest thermal efficiency. The optimal values of the design variables of the $scCO_2$ WHR unit can be easily calculated once the typical design constraints for the system components are set, and these are: i) $\Delta T_{pinch,reg.} = 15$ °C, ii) $\Delta T_{approach,heater} = 20$ °C, iii) $P_{min} = 74$ bar, iv) $P_{max} = 400$ bar, v) $T_{min} = 283$ K.

Cooler. The heat exchanger geometry chosen for the cooler is similar to that conceived by a major engine manufacturer for the heat transfer equipment of intercooled recuperated engines [5]. The cooler consists of six different modules placed in parallel as shown in Fig. 8. Each heat exchanger is formed by multiple U-shaped tubes arranged in a staggered configuration and brazed at their ends into two manifolds. Proper construction materials are titanium alloys, as the Ti-6Al-4V alloy proposed in Ref. [5], thus its properties are input to the preliminary sizing calculations. In order to minimize the pressure loss on the air side of the heat exchanger, the tubes are assumed to have an elliptical profile, whose main axis (D_{max}) is aligned with the air flow direction. For the case at hand, D_{max} is equal to 9 mm, while the minor axis of the profile (D_{min}) measures 4.5 mm. The aspect ratio (Ar) of the tube cross-section is thus equal to 2. The adoption of a more flattened shape is not a viable solution for the considered application, although this would allow for a reduction of the pressure drop over the cooling air side. Profiles characterized by a higher value of Ar would lead to an unrealistically large thickness of the tubes (s_{tube}), due to the relatively high pressure of CO_2 and to the mechanical stress amplification occurring in the two pipe corners, where profile curvature is minimum. Application of the Von Mises criterion at the two ends of the major axis of the ellipse results in a tube thickness that is proportional, to a first approximation, to Ar^2, being

$$s_{tube} = max\left(\frac{P_{CO_2}\cdot D_{max}}{2\sigma_{metal}}\sqrt{3+Ar^4-3Ar^2}, 0.3mm\right) \quad (1)$$

where σ_{metal} is the allowable yield stress of the material.

The conventional design problem of heat exchangers entails determining the surface area required to transfer a specified thermal duty, for a given temperature and mass flow rate of the inlet flow streams. On the contrary, the design specifications in this case are: the pressure drop in the cooling air flow ($\Delta P_{\text{air,cooler}}$) and the space limitations within the engine nacelle. At this stage of the research, the most suitable design variable is arguably $\Delta P_{\text{air,cooler}}$, since a reasonable estimate for its value can be specified, based on the state-of-art design of the intercooler for IRE systems [5]. Accordingly, $\Delta P_{\text{air,cooler}}$ has been set to 6% of the total pressure at inlet. The maximum frontal area of the cooler depends, to a first approximation, on the value of $A_{2,\text{tot}}$, see Fig. 9. The unknowns of the preliminary design problem are the mass flow rate of the cooling air $\dot{m}_{\text{coolant}}$ and of the working fluid $\dot{m}_{\text{CO}_2}$, as well as the cooler heat transfer rate $\dot{Q}_{\text{cooler}}$. These values can be determined by solving iteratively a non-linear system of equations, which involves the conservation equations of mass and energy for the fan duct, and simplified relations for the prediction of the thermo-hydraulic characteristics of the heat exchanger. More in detail, the ad-hoc numerical procedure developed to perform the preliminary design of the cooler includes the following main steps:

1. an initial guess for $\dot{m}_{\text{coolant}}$ is provided. Since the fan operating conditions are inputs of the problem, this permits to estimate the mass flow rate of the air circulating in the main fan duct $\dot{m}_{\text{duct}}$ by solving a simple mass balance;
2. the specific thermodynamic properties and velocity of the air stream at station 2,2s in Fig. 9 are estimated by assuming that the fluid undergoes an isentropic expansion process and the cooler outlet pressure is therefore $P_0 - \Delta P_{\text{air,cooler}}$. The area required to accommodate this flow ($A_{2,2\text{s}}$) is then calculated as $A_{2,2\text{s}} = \dot{m}_{\text{duct}}/(\bar{\rho}_{2,2\text{s}} \cdot v_{2,2\text{s}})$;
3. the frontal area of the cooler ($A_{2,1\text{s}}$) is evaluated by subtracting $A_{2,2\text{s}}$ from the original size of the by-pass duct, i.e., $A_{2,\text{tot}}$. Hence, it is possible to determine the number of tubes along the heat exchanger height and their average length, given D_{min} of the adopted elliptical profile and the pitch among the tubes, here assumed equal to 15.4mm, as in [18]. The geometry of the cooler results fully specified except for the number of tubes along the flow direction of the cooling air ($N_{\text{tube rows}}$);
4. The sizing of the cooler is then completed by solving the implicit and non-linear equation system

$$\dot{Q} = F \cdot U \cdot A(N_{\text{tube rows}}) \cdot \Delta T_{lm} \tag{2a}$$
$$\dot{Q} = \dot{m}_{\text{coolant}} \cdot \Delta h_{\text{coolant}}(T_{\text{out,coolant}}) \tag{2b}$$
$$\dot{Q} = \dot{m}_{\text{CO}_2} \cdot \Delta h_{\text{CO}_2} \tag{2c}$$
$$\Delta P_{\text{air,cooler}} = \frac{1}{2} \cdot f \cdot N_{\text{tube rows}} \cdot \bar{\rho} \cdot \bar{v}^2_{\text{coolant}} \tag{2d}$$

   for unknowns $\dot{Q}, T_{\text{out,coolant}}, N_{\text{tube rows}}, \dot{m}_{\text{CO}_2}$. F is the correction factor of the logarithmic mean temperature difference (ΔT_{lm}) to account for the departure of the actual cooler geometry from that of a counter-current heat exchanger. The value of F is estimated through a numerical correlation calibrated for cross-flow heat exchanger with one fluid unmixed. U and the pressure drops are determined on the basis of the average thermodynamic properties of the streams in the cooler and of empirical relations involving the typical dimensionless groups of heat transfer problems, namely the Reynolds, the Prandtl and the Nusselt number. The correlations reported in Ref. [17] are used to predict the heat transfer coefficient and the friction factor (f) in the CO_2 stream, whereas those documented in Ref. [18] are employed to estimate the same quantities for the cooling air.
5. Given the thermodynamic conditions at the cooler outlet and $A_{2,1\text{s}}$, a new value of $\dot{m}_{\text{coolant}}$ is computed. If this differs form the previous estimate, the calculations of steps 1-5 are repeated until the average change of $\dot{m}_{\text{coolant}}$ is lower than the specified tolerance.

Heater The heater consists of several heat exchangers modules, similar to those adopted for the cooler. Simple geometrical relations derived on the basis of the space constraints allow for the estimation of the frontal area of the heater modules, the number of tubes along the heat exchanger height, and their average length. The estimate of the number of tubes along the flow direction of the exhaust requires the solution of a non-linear system of equations similar to (2). However, in this case and that of the regenerator, the main design specification is the heat transfer rate (instead of the pressure drop), while the temperature and mass flow rate of the inlet streams are inputs. Thus, the preliminary design problem can be reduced to the non-linear system formed by equation (2b)-(2d). The pressure loss in the exhausts is subsequently estimated with a relation equivalent to (2d). Similarly, the correlations for the prediction of the heat transfer coefficients of the cold and hot stream are the same adopted for the preliminary design of the cooler. Due to the higher operating temperature of the heater with respect to the cooler, a lower value of the material yield stress is assumed. As documented in Ref. [5], σ_{metal} is taken equal to 280 MPa.

Regenerator. The regenerator selected for this application is a printed circuit heat exchanger, because it is extremely com-

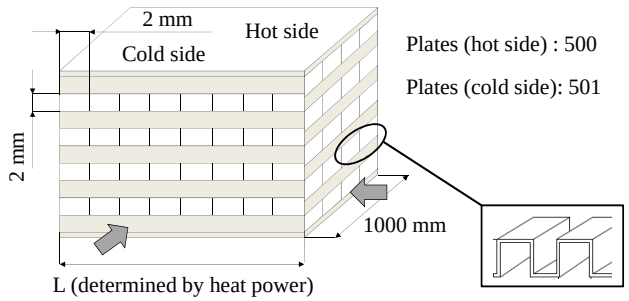

FIGURE 10. **Geometry and configuration of the printed circuit regenerator of the scCO$_2$ waste heat recovery unit.**

pact and capable of sustaining high pressure, and because information about its use in terrestrial applications is available. Such choice is arguably sub optimal, given that in stationary power plant the weight of the heat exchangers is not a primary concern. The main geometrical characteristics of the regenerator are reported in Fig. 10. The plate length (L) is the unknown parameter of the sizing problem and it is determined by matching the specified heat transfer duty. The additional information required for the preliminary design of this component is the value of the global heat transfer coefficient and of the plate thickness; the heat transfer coefficient is estimated according to the relations reported in Ref. [19], while the plate thickness is evaluated as

$$s = \max((P_{\max} - P_{\min}) \cdot \frac{D}{\sigma_{\text{metal}}}; 0.5 \text{ mm}), \qquad (3)$$

The allowable yield stress (σ_{metal}) of the material, i.e. ,the Ti-6Al-4V alloy, is taken equal to 300 MPa. No space constraints are considered for the regenerator. It is arbitrarily assumed that it can be properly accommodated in the aircraft fuselage.

3.2 Results

The SFC resulting from the simplified simulation of the CCE is 54.7 kg/kN/h, while the total thrust is 72.2 kN, of which 2.8 kN are provided by the WHR unit. The reduction of SFC with respect to the SFC of the GE90-94B is about 2.8%, thus nearly one of order of magnitude lower than the value predicted by the sole thermodynamic cycle analysis. In addition, the model does not take into account the additional fuel consumption due to the weight of scCO$_2$ WHR unit, which is about 3 tons. On the basis of the simplified relation proposed in Ref. [16] the weight of the WHR unit would cause an SFC increase of 4 %, which would disqualify further development of the configuration whereby the WHR unit is an add-on to a conventional turbofan for a conventional aircraft. However, the analysis of the results and of the assumptions provide further insights that suggest further investigation.

According to the simulation results reporter in Table 5, the cooler is the most critical component of the system: the relatively low ΔT_{lm} and the poor heat transfer coefficient of the cooling air side determine large values of the required heat transfer surface. Consequently, the tube bundle of each cooler module features a large number of tubes in parallel. This, in turn, leads to low CO$_2$ velocity inside the tubes, which also negatively affects the global heat transfer coefficient. Despite the large heat transfer area and weight, the thermal duty of the cooler is only 1.6 MW, which poorly compares with the values reported in Fig. 4. The low duty of the cooler, due to the various constraints, limits the CO$_2$ mass flow rate circulating in the WHR unit, and consequently the thermal power that can be recovered from the gas turbine exhaust. The calculated duty of the heater is 2.6 MW (see Table 5), which is less than half of the value of 7 MW that can be deduced from Fig. 5. The heat duty of the heater is almost twice the one of the cooler, while its weight is less than half of that of the cooler. The main reason for the better predicted performance of the heater compared to that of the cooler is the higher heat transfer coefficient in both the cold and the hot side. In particular, the heat transfer coefficient of the CO$_2$ side is very high, being more than 2400 W/m^2/K. Additionally, the temperature difference between the hot and cold side of the heater is much higher compared to that of the cooler. Similar considerations are valid for the regenerator. Its large weight if compared to that of the heater, albeit a 20% lower heat transfer rate, is mainly due to i) the smaller ΔT_{lm}, namely 41 K in lieu of 68 K in the heater, and ii) the lower capability of printed circuit HEXs in handling high pressure if compared to tubular heat exchangers.

	Cooler	Regenerator	Heater
$\dot{m}_{\text{hot}}$ (kg/s)	7.0	7.0	54.8
$\dot{m}_{\text{cold}}$ (kg/s)	87.1	7.0	7.0
$T_{\text{hot, inlet}}$ (K)	324.3	574.0	778.4
$T_{\text{hot, outlet}}$ (K)	283.0	324.3	734.9
$T_{\text{cold, inlet}}$ (K)	267.4	309.3	481.8
$T_{\text{cold, outlet}}$ (K)	284.1	481.8	758.4
h_{hot} (W/m^2/K)	131	677	318
h_{cold} (W/m^2/K)	148	343	2415
ΔP_{hot} (%)	<1	2.2	2.1
ΔP_{cold} (%)	6	<1	1.4
# of tubes/channels	37,067	29,175 (hot side)	6,506
Thermal duty (kW)	1,598	2,119	2,620
Weight (kg)	1,608	920	692

TABLE 5. **Estimated operating conditions and main characteristics of the three heat exchangers of the scCO$_2$ WHR unit for the GE90-94B turbofan.**

A more detailed investigation of the cooler configuration,

e.g. its positioning on-board of the aircraft, and geometry, e.g. the shape of tube profile or the number of passes of the CO_2 stream, is needed to assess the actual potential of the CCE. Furthermore, future analysis must reconsider also the design variables of the $scCO_2$ cycle, here kept as constant as very preliminary estimation. To make an example, the minimum temperature T_{min} has a great impact on the HEX size, and it can be optimized to reduce the required heat transfer surface.

4 CONCLUSIONS

A new concept for the propulsion system of long-haul aircraft has been preliminarily investigated. This engine concept is based on a combined cycle configuration whereby the thermal energy of the exhaust of the gas turbine powers a closed-cycle $scCO_2$ waste heat recovery unit. Simplified thermodynamic calculations have been performed in order to evaluate the potential of the idea in terms of thermal efficiency. This assessment considers the inter-refrigerated recuperated cycle configuration as benchmark, because it has been extensively studied in the recent past. In addition, as a probing exercise, the simplified design of a system formed by a GE90-94B turbofan engine and a $scCO_2$ waste heat recovery unit has been carried out.

The results of the investigation reported here suggest the following conclusions:

1. the thermodynamic quality of the combined cycle configuration is higher than that of the intercooled recuperated configuration;
2. thermodynamic calculations show that the optimal thermodynamic performance of the combined cycle engine is expected to occur at OPR values higher than that of current turbofan engines. This result suggests that heat recovery by means of a $scCO_2$ bottoming unit might be attractive also for next-generation aero gas turbines;
3. simplified calculations aimed at designing a $scCO_2$ waste heat recovery unit as an add-on for GE90-94B turbofan show that the estimated SFC reduction of 2.8% is insufficient, if the additional weight of the unit, about 3 tons per aircraft engine, is factored in. This is however caused by i) the strong limitations of the add-on configuration due to the limited space available within a conventional nacelle, ii) the adverse effects of locating the cooler in the fan duct and iii) the lack of proper heat exchanger technology for this highly unconventional application;
4. the cooler is the most critical component of the $scCO_2$ system in terms of volume and weight. As a first attempt, the heat exchanger geometry developed for the intercooler of the intercooled recuperated aero engines has been considered. However, such configuration turns out to be largely sub optimal.

In order to duly assess the potential of the combined cycle aero engine, future research will investigate with more detailed simulations: innovative aircraft-propulsion integration configurations that allow to better exploit the thermal energy at the gas turbine outlet, different configurations of the heat recovery unit and innovative and specialized heat exchangers.

NOMENCLATURE

Acronyms

CCE Combined Cycle Engine
HEX Heat Exchanger
HPC High pressure compressor
HPT High pressure turbine
IRE Intercooled-recuperative engine
LPC Low Pressure Compressor
OPR Overall Pressure Ratio (-)
NTU Number of Transfer Units, cooler
ORC Organic Rankine Cycle
SFC Specific Fuel Consumption (kg/kNh)
TIT Turbine Inlet Temperature (K)
WHR Waste Heat Recovery

Symbols

A Area (m^2)
Ar Aspect ratio (-)
C_{min} Smallest fluid heat capacity (W/K)
D Tube diameter (mm)
F Thrust (kN)
h Heat transfer coefficient ($W/m^2/K$)
W Weight (kg)
$\dot{m}$ Mass flow rate kg/s)
P Pressure (MPa)
Q Heat exchanger power (kW)
s Tube thickness (mm)
T Temperature (K)
U Global heat transfer coefficient ($W/m^2/K$)
V_∞ Cruise velocity (m/s)
PW Mechanical power of the WHR unit (kW)

Greek letters

ΔP Pressure drop (MPa)
ΔT Temperature variation (K)
ΔT_{lm} Logarithmic mean temperature (K)
η_{conv} Conversion efficiency (-)
λ Thermal conductivity (W/m/K)
ρ Density (kg/m^3)
σ Metal Stress (MPa)

Subscripts

CO_2 WHR unit property
cold Core nozzle property

cooler Cooler property
core Core nozzle property
engine Turbofan property
fan Fan nozzle property
heater Heater property
hot Fan nozzle property
inlet Inlet property (for HEX)
limit Upper limit
max Maximum value (forCO_2
min Maximum value (for CO_2)
metal Metal property
outlet Outlet property (for HEX)
pinch Pinch point (for HEX)
reg Regenerator stress

REFERENCES

[1] German Aerospace Center, 2008. Analyses of the European air transport market. Annual report, European Commission, Bruxelles.

[2] Kyprianidis, K. G., 2011. *Future aero engine designs: an evolving vision*. Intech, ch. 1, pp. 1–23.

[3] McDonald, C., and Rodgers, C., 2009. "Heat exchanged propulsion gas turbines: a candidate for future lower SFC and reduced emission military and civil aeroengines". In Proceedings of ASME Turbo Expo 2009, Vol. 1, IGTI, ASME, pp. 33–49.

[4] ARTTIC, with contribution of all partners, 2011. Newac - new aero engine core concepts. Technical Report NEWAC-ART-DEL-FAR-R1.0, ARTTIC, September. Publishable final activity report.

[5] Gonser, H., 2008. "Untersuchungen zum Einsatz von Wärmetauschern in zivilen turboflugtriebwerken". PhD thesis, Institut für Luftfahrtantriebe der universität Stuttgard, Stuttgard, Oct.

[6] Perullo, C., Mavris, D., and Fonseca, E., 2013. "An integrated assessment of an organic Rankine cycle concept for use in onboard aircraft power generation". In Proceedings of ASME Turbo Expo 2013, Vol. 2, IGTI, ASME, pp. V002T01A028–8.

[7] Angelino, G., 1968. "Carbon dioxide condensation cycles for power production". *J. Eng. Power,* ***90***(3), July, pp. 287–295.

[8] Invernizzi, C. M., 2013. *Closed power cycles. Thermodynamic Fundamentals and Applications*, Vol. 11 of *Lecture Notes in Energy*. Springer-Verlag London.

[9] Dostal, V., Hejzlar, P., and Driscoll, M., 2006. "High-performance supercritical carbon dioxide cycle for next-generation nuclear reactors". *Nucl. Technol.,* ***154***(3), June, pp. 265–282.

[10] Persichilli, M., Held, T., Hostler, S., Zdankiewicz, E., and Klapp, D., 2011. "Transforming waste heat to power through development of a CO_2-based power cycle". In Proceedings of Electric Power Expo 2011, pp. 1–8.

[11] Visser, W. P. J., and Broomhead, M. J., 2000. "GSP, a generic object-oriented gas turbine simulation environment". In Proceedings of ASME Turbo Expo 2000, Vol. 1, IGTI, ASME, pp. V001T01A002–8.

[12] Visser, W., 2015. "Generic analysis methods for gas turbine engine performance". PhD thesis, Delft University of Technology, Delft, The Netherlands, Jan.

[13] MathWorks, 2013. Matlab, release 2013b. Software.

[14] Boyce, M. P., 2012. *Gas turbine engineering handbook*, 4 ed. Elsevier, December.

[15] Kurzke, J., 2003. "Aero-engine design: A state of the art - preliminary design". In *Von Karman Institute Lecture Series*. Von Karman Institute, April.

[16] Cumpsty, N., 2015. *Jet Propulsion: A Simple Guide to the Aerodynamic and Thermodynamic Design and Performance of Jet Engines*, 3 ed. Cambridge University Press, Cambridge, ch. 7, p. 94.

[17] Sogni, A., and Chiesa, P., 2014. "Calculation code for helically coiled heat recovery boilers". *Energy Procedia,* ***45***(5), January, pp. 492–501.

[18] Ibrahim, T. A., and Gomaa, A., 2009. "Thermal performance criteria of elliptic tube bundle in crossflow". *Int. J. Therm. Sci.,* ***48***(11), November, pp. 2148–2158.

[19] Pierobon, L., Benato, A., Scolari, E., Haglind, F., and Stoppato, A., 2014. "Waste heat recovery technologies for offshore platforms". *Appl. Energy,* ***136***, January, pp. 228–241.